

FILE COPY  
NO 8CASE FILE  
COPY

RM E50G24



## RESEARCH MEMORANDUM

FUNDAMENTAL FLAME VELOCITIES OF PURE HYDROCARBONS

I - ALKANES, ALKENES, ALKYNES

BENZENE, AND CYCLOHEXANE

By Melvin Gerstein, Oscar Levine  
and Edgar L. WongLewis Flight Propulsion Laboratory  
Cleveland, OhioTHIS DOCUMENT IS ON LOAN FROM THE FILES OF  
NATIONAL ADVISORY COMMITTEE FOR AERONAUTICS  
LANGLEY AERONAUTICAL LABORATORY  
LANGLEY FIELD, HAMPTON, VIRGINIARETURN TO THE ABOVE ADDRESS.  
REQUESTS FOR PUBLICATIONS SHOULD BE ADDRESSED  
AS FOLLOWS:NATIONAL ADVISORY COMMITTEE FOR AERONAUTICS  
1512 H STREET, N. W.  
WASHINGTON 25, D. C.NATIONAL ADVISORY COMMITTEE  
FOR AERONAUTICS

WASHINGTON

September 28, 1950

NATIONAL ADVISORY COMMITTEE FOR AERONAUTICS

RESEARCH MEMORANDUM

FUNDAMENTAL FLAME VELOCITIES OF PURE HYDROCARBONS

I - ALKANES, ALKENES, ALKYNES,  
BENZENE, AND CYCLOHEXANE

By Melvin Gerstein, Oscar Levine  
and Edgar L. Wong

SUMMARY

The flame velocities of 37 pure hydrocarbons including normal and branched alkanes, alkenes, and alkynes, as well as benzene and cyclohexane, together with the experimental technique employed are presented.

The normal alkanes have about the same flame velocity from ethane through heptane with methane being about 16 percent lower. Unsaturation increases the flame velocity in the order of alkanes, alkenes, and alkynes. Branching reduces the flame velocity.

INTRODUCTION

The rate of flame propagation through hydrocarbon-air mixtures has been intensively studied from both the theoretical and applied approach. Investigators attempting to establish the mechanism of flame propagation through thermal and diffusion theories have encountered a lack of consistent flame velocities for a variety of fuels. These investigators were usually restricted to a consideration of the variation of flame velocity with fuel concentration and were unable to compare different types of fuel. Investigators attempting to correlate flame velocities with the performance of fuels in combustors in applied research have been unable to determine whether a correlation exists because of the inherent inconsistency in the flame-velocity data found in the literature.

The research reported herein was undertaken at the NACA Lewis laboratory to provide a self-consistent set of flame-velocity measurements for use in correlations with propagation theories and combustor-performance results.

## APPARATUS AND PROCEDURE

Figure 1 is a schematic diagram of the experimental apparatus showing the tube method used. The vaporized liquid or gaseous compound was admitted into the evacuated system to prepare a combustible mixture of hydrocarbon and air. The hydrocarbon pressure was obtained from the absolute manometer. In order to reduce meniscus effects, the manometer tubing used in the measurement of pressures below 100 millimeters mercury had a diameter of 14 millimeters. Pressures in this range were read with the aid of a cathetometer with a precision of  $\pm 0.02$  millimeter mercury. Air was admitted to the system after carbon dioxide and water vapor had been removed by Ascarite and anhydrous magnesium perchlorate, respectively. The total pressure of the mixture was recorded. The hydrocarbon-air mixture contained in the 5-liter flask was then agitated by means of a motor-driven bellows stirrer. Infrared absorption spectra of samples withdrawn after 5 and 15 minutes of stirring indicated that a 5-minute period was sufficient to yield a completely homogeneous mixture. The hydrocarbon-air mixture was then transferred to the horizontal flame tube by means of a modified Toepler pump. The barometer indicated that the mixture within the flame tube was at atmospheric pressure. A sufficient period of time (usually 1 min) was allowed for the mixture within the flame tube to become quiescent. Immediately prior to ignition, the flame tube was opened to the atmosphere at both ends and ignition was accomplished by means of a small alcohol lamp.

The flame tube consisted of a 2.8-centimeter outside-diameter pyrex tube, 57 centimeters in length. A 35/25 semiball joint was attached to each end for connection to the vacuum apparatus. The end of the flame tube at which ignition was effected contained an 8-millimeter orifice, which was the size calculated by Guénoc'h (reference 1) to reduce pressure disturbances in the tube. After a series of tests, an additional orifice, 1.7 millimeters in diameter, was placed in the end of the tube toward which the flame advanced in order to increase the uniformity of flame travel.

Coward and Payman (reference 2) related the fundamental flame velocity  $U_f$  to the linear observed flame velocity  $U_o$  by the equation

$$U_f = (U_o - U_g)(A_t/A_f) \quad (1)$$

The fundamental flame velocity  $U_f$  is that velocity component normal to any tangent to the flame surface; it is a function of hydrocarbon type and concentration and is independent of the geometry

1382  
of the experimental apparatus. The linear or spatial observed flame velocity  $U_o$  is that velocity component normal to the cross-sectional plane of the tube; it is a function of hydrocarbon type and concentration and is entirely dependent on the geometry of the experimental apparatus. The gas velocity  $U_g$  is the mean velocity of the unburned gas set in motion ahead of and away from the advancing flame. The terms  $A_t$  and  $A_f$  are the cross-sectional area of the tube and the surface area of the flame, respectively.

The spatial flame velocity  $U_o$  was measured by means of photocells connected to an electronic timer. Because the time interval measured was about 0.1 second, the timer had to accurately measure time intervals as small as 0.003 second to obtain a desired precision of  $\pm 1.5$  percent. The photocells 6 inches apart acted as switches, to control the flow of current from the 10,000-cycle oscillator into the pulse counter. The number of pulses recorded on the counter was directly proportional to the time interval between the excitation of the two photocells. The timer circuit was chosen because of its rapid response. In order to test the absolute accuracy of the timer, an oscillograph was placed in a parallel circuit with the timer and high-speed motion pictures were taken of the oscillograph screen as the flame progressed in the tube. The time markings on the film between the two points of excitation caused by the flame's passing the two photocells agreed with the recorded time interval within  $\pm 1.5$  percent.

One of the primary difficulties with previous measurements of spatial flame velocities in tubes has been the uncertainty of the uniformity of the flame movement within the tube. In order to establish this uniformity, the flame was photographed with a rotating drum camera from which the shutter had been removed. Because the film motion was held constant and directed at right angles to the direction of flame travel, a straight-line trace on the film was an indication that the flame velocity had also been constant. Traces taken for representative hydrocarbons over the velocity range in this investigation indicated that the flame velocity remained constant in the region between the photocells. In figure 2 a typical straight-line trace is shown with the directions of film and flame travel as indicated. The slope of the line is dependent on the fuel type and concentration.

The gas velocity term  $U_g$  was determined by experimental measurement of the volumetric rate of gas flow within that part of the flame tube toward which the flame was advancing. The volumetric rate of flow was determined from photographs of the progressive

growth of a soap bubble blown from a tube connected to the flame tube. This volumetric rate of flow divided by the cross-sectional area of the flame tube  $A_t$  yielded a mean value for the gas velocity. In order to determine  $U_g$ , a glass tube bent at right angles so that the open end faced downward was inserted into the small orifice. The glass tube had a gradually increasing diameter from 1.5 to 10 millimeters. The dimensions of this tube were experimentally determined to insure that its use would not affect the area or velocity of the flame. Immediately prior to ignition, a soap film was placed across the large end of the glass tube. As the flame progressed in the tube, a soap bubble was formed by the ejection of gas from that part of the tube towards which the flame was advancing. The soap bubble and an oscilloscope screen were photographed simultaneously at 64 frames per second. The volume of the soap bubble was calculated at the two points of excitation on the oscilloscope screen caused by the flame's passing the two photocells. A typical frame from a photographic record is shown in figure 3. The increase in volume of the soap bubble and a time reading obtained simultaneously with the electronic timer yielded a value of the volumetric rate of gas flow. The variation of  $U_g$  with the spatial flame velocity  $U_o$  is shown in figure 4. The data presented were taken for three different types of fuel covering a wide range of spatial flame velocities. A straight line faired through the data over a range of spatial flame velocities from 70 to 150 centimeters per second can be represented by

$$U_g = 0.236 U_o - 10.47 \quad (2)$$

Although there is considerable scatter in the data, the gas-velocity correction applied to the observed velocity  $U_o$  is a small one so that none of the deviations produce more than 2- to 3-percent error in the final result.

The cross-sectional area of the tube  $A_t$  was obtained by direct measurement of the internal diameter of the tube.

The flame-surface area  $A_f$  was obtained from photographs of the flame surface (fig. 5). The area  $A_f+A_2$  of the surface bounded by the flame surface and a straight line joining the two points at which the flame touches the tube was calculated by the method of Coward and Hartwell (reference 3). In order to get the surface area of the flame itself  $A_f$ , the element of area  $A_2$  was calculated by assuming that this element was half of a prolate spheroid. The areas  $A_f$  and  $A_2$  were constants for all the hydrocarbons studied in this research.

In order to check the reproducibility of the experimental procedure, n-hexane was periodically tested during the investigation. At no time did the values obtained for this hydrocarbon differ by more than 2 percent. At least three determinations for the observed velocity  $U_o$  were made for each mixture concentration studied. The flame velocities reported here are average values and have a precision of  $\pm 2$  percent.

#### RESULTS AND DISCUSSION

The flame velocities of 37 pure hydrocarbons including normal and branched alkanes, alkenes, and alkynes, as well as cyclohexane and benzene are summarized in table I. The observed linear velocity  $U_o$  and the corrected linear velocity  $U_o - U_g$  are given together with the maximum calculated fundamental flame velocity  $U_f$ . Where available, the purity and the source of the hydrocarbons are given.

The variation of the fundamental flame velocity with fuel concentration is presented in figure 6 for the normal alkanes from methane through heptane. The stoichiometric concentration is indicated by arrows. In general, the maximum flame velocity occurs in mixtures containing 10 to 30 percent excess fuel. Similar curves for the 1-alkenes, 1-alkynes, branched alkanes, branched 1-alkenes, cyclohexane, benzene, and other alkynes are shown in figures 7 to 12.

A summary of the maximum flame velocities from the preceding figures is shown in figures 13 to 15. In figure 13 it can be seen that the normal alkanes from ethane through heptane have approximately the same flame velocity; methane is about 16 percent lower. Unsaturation increases the maximum flame velocity. In general, the alkynes have the highest flame velocities with the alkenes intermediate and the alkanes lowest. The increase in maximum flame velocity is most pronounced in the compounds of low molecular weight; the effect decreases as the number of carbon atoms in the chain increases.

The effect of branching on flame velocity can be seen in figures 14 and 15. In every case, branching appears to lower the flame velocity although many of the changes are within the experimental error of  $\pm 2$  percent. As with unsaturation, the reduction in flame velocity due to branching is most pronounced in the hydrocarbons of low molecular weight.

## CONCLUSIONS

From the study of flame velocities for 37 pure hydrocarbons including normal and branched alkanes, alkenes, and alkynes, as well as cyclohexane and benzene, the following conclusions are drawn:

1. Unsaturation increases flame velocities of the hydrocarbons in the increasing order: alkanes, alkenes, and alkynes.
2. Branching reduces the flame velocity of a hydrocarbon.

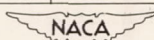
Lewis Flight Propulsion Laboratory,  
National Advisory Committee for Aeronautics,  
Cleveland, Ohio.

## REFERENCES

1. Guénoche, Henri, Manson, Numa, et Monnot, Gustave: La propagation uniforme d'une déflagration dans un tube cylindrique lisse. *Comptes Rendus*, T. 226, Jan. 12, 1948, p. 163-164.
2. Coward, H. F., and Payman, W.: Problems in Flame Propagation. *Chem. Rev.*, vol. 21, no. 3, Dec. 1937, pp. 359-366.
3. Coward, H. F., and Hartwell, F. J.: Studies in the Mechanism of Flame Movement. Part II. The Fundamental Speed of Flame in Mixtures of Methane and Air. *Jour. Chem. Soc. (London)*, pt. II, 1932, pp. 2676-2684.

TABLE I - SUMMARY OF RESULTS

Fuel	Source	Estimated purity (percent)	Maximum $U_o$ (cm/sec)	Maximum $U_o - U_g$ (cm/sec)	Maximum $U_f$ (cm/sec)	Volume percent fuel at maximum $U_f$
Methane	M <sup>1</sup>	99	84.5	75.0	33.8	9.96
Ethane	P <sup>2</sup>	99.9	102.8	89.0	40.1	6.28
Propane	P	99	99.5	86.5	39.0	4.54
Butane	P	99	96.2	84.0	37.9	3.52
Pentane	NACA <sup>3</sup>	99.3	98.0	85.3	38.5	2.92
Hexane	NACA	97	98.0	85.3	38.5	2.51
Heptane	NACA	----	98.3	85.6	38.6	2.26
2-Methylpropane	P	99	87.5	77.3	34.9	3.48
2,2-Dimethylpropane	P	99	83.0	73.9	33.3	2.85
2-Methylbutane	NACA	99.4	92.5	81.1	36.6	2.89
2,2-Dimethylbutane	NACA	98	90.0	79.2	35.7	2.43
2,3-Dimethylbutane	NACA	----	91.7	80.5	36.3	2.45
2,2,3-Trimethylbutane	NACA	----	90.5	79.6	35.9	2.15
2-Methylpentane	NACA	99.3	93.0	81.5	36.8	2.46
3-Methylpentane	NACA	98	92.7	81.3	36.7	2.48
2,3-Dimethylpentane	NACA	----	92.2	80.9	36.5	2.22
2,4-Dimethylpentane	P	99	89.9	79.2	35.7	2.17
Ethene	O <sup>4</sup>	99.5	184.5	151.4	68.3	7.40
Propene	P	99	113.4	97.1	43.8	5.04
1-Butene	P	99	111.5	95.7	43.2	3.87
1-Pentene	NACA	----	110.0	94.5	42.6	3.07
1-Hexene	NACA	----	108.5	93.4	42.1	2.67
2-Methyl-propene	P	----	95.0	83.1	37.5	3.83
2-Methyl-1-butene	NACA	----	99.5	86.5	39.0	3.12
3-Methyl-1-butene	NACA	----	106.9	92.1	41.5	3.11
2-Ethyl-1-butene	NACA	----	100.3	87.1	39.3	2.65
2-Methyl-1-pentene	NACA	----	101.2	87.8	39.6	2.80
4-Methyl-1-pentene	NACA	----	104.0	89.9	40.5	2.62
Propyne	NACA	98	189.1	154.9	69.9	5.86
1-Butyne	NACA	99.7	155.0	128.9	58.1	4.36
1-Pentyne	NACA	----	140.0	117.4	52.9	3.51
1-Hexyne	NACA	----	127.0	107.5	48.5	2.97
4-Methyl-1-pentyne	NACA	----	116.9	99.8	45.0	2.87
2-Butyne	NACA	----	135.6	114.1	51.5	4.36
3-Hexyne	NACA	----	118.0	100.6	45.4	3.05
Cyclohexane	----	----	98.4	85.7	38.7	2.65
Benzene	----	----	104.5	90.3	40.7	3.34

<sup>1</sup>The Matheson Company, Inc.<sup>2</sup>Phillips Petroleum Company.<sup>3</sup>Prepared jointly by National Bureau of Standards and NACA.<sup>4</sup>Ohio State University Research Foundation, A.P.I. Research Project 45.

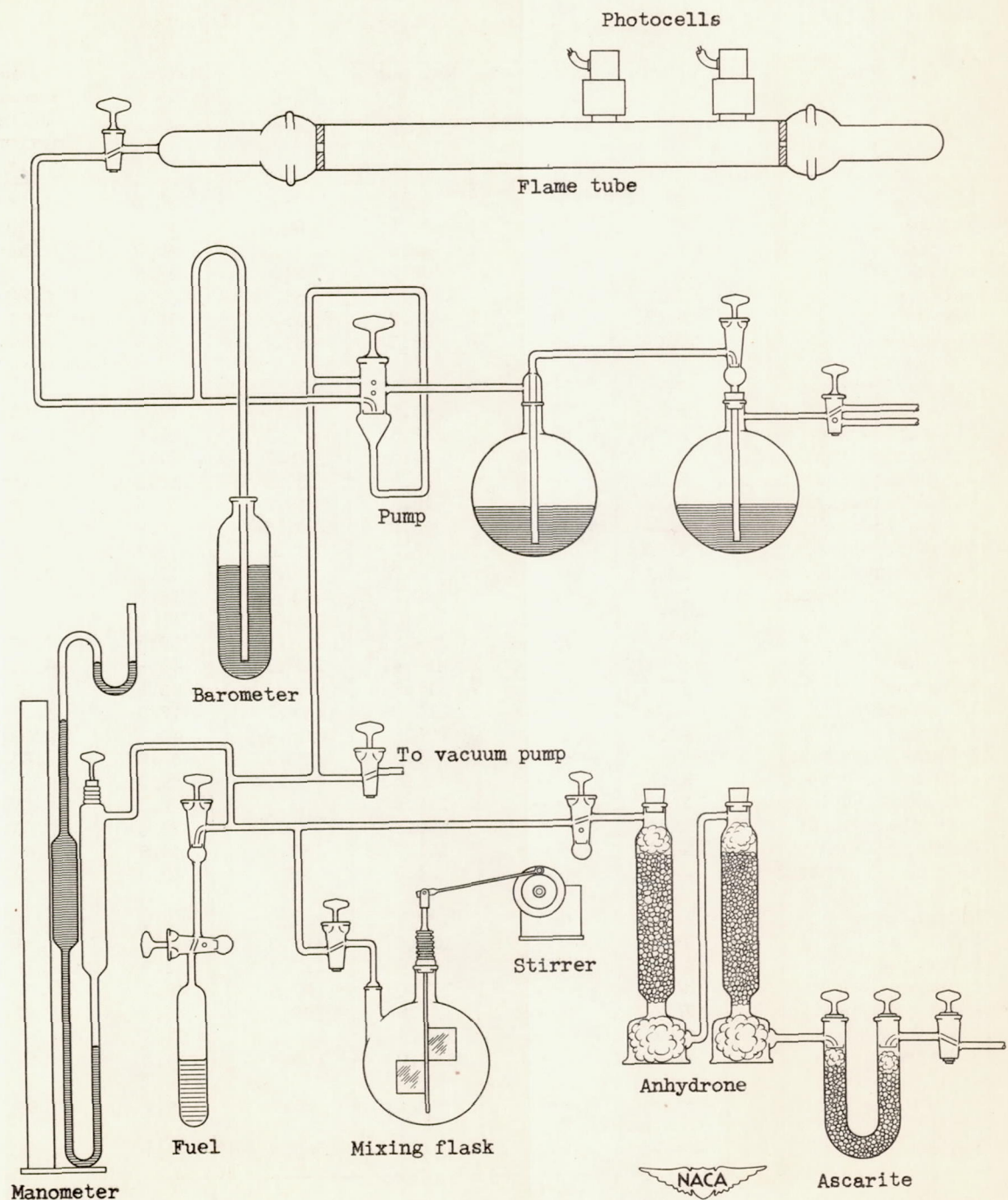


Figure 1. - Flame-speed apparatus.

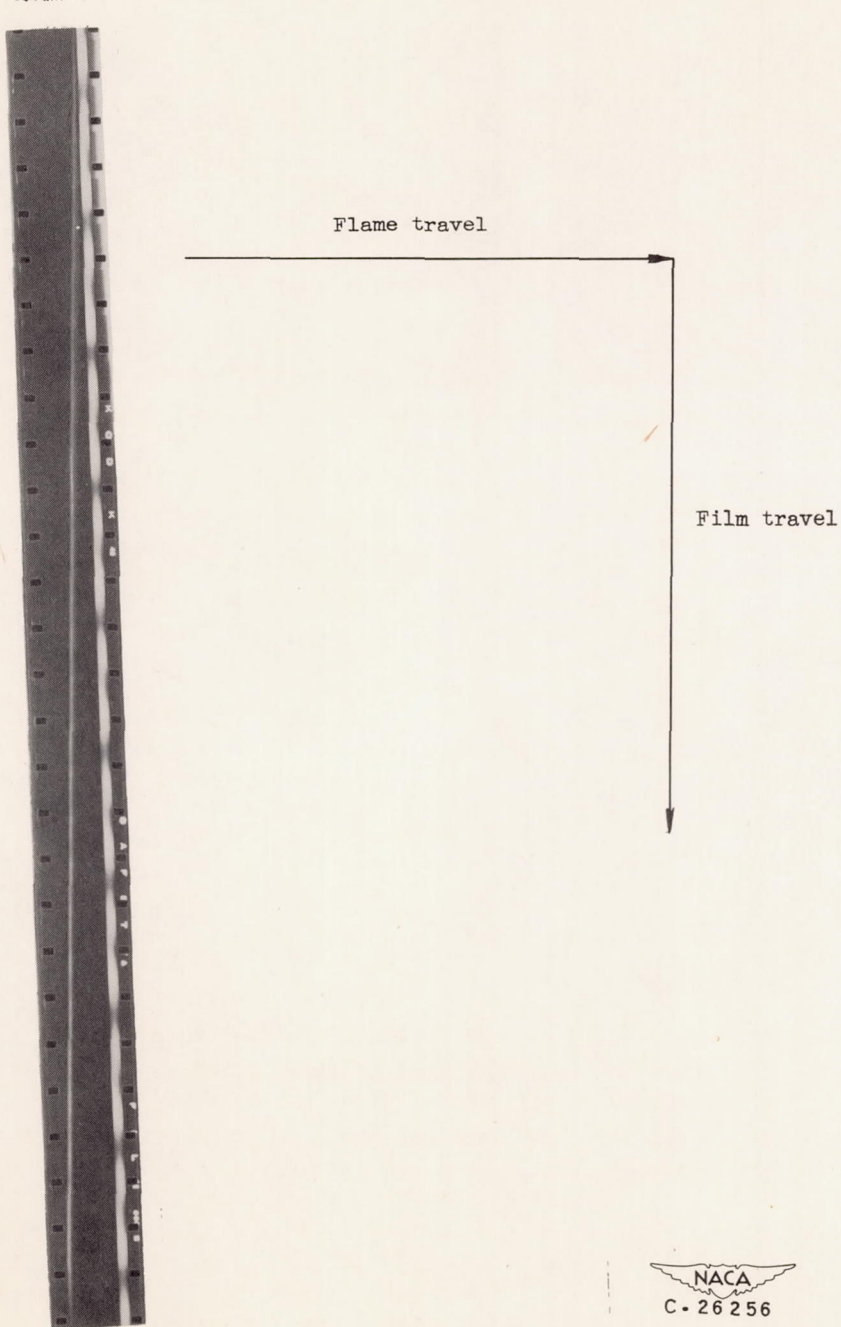
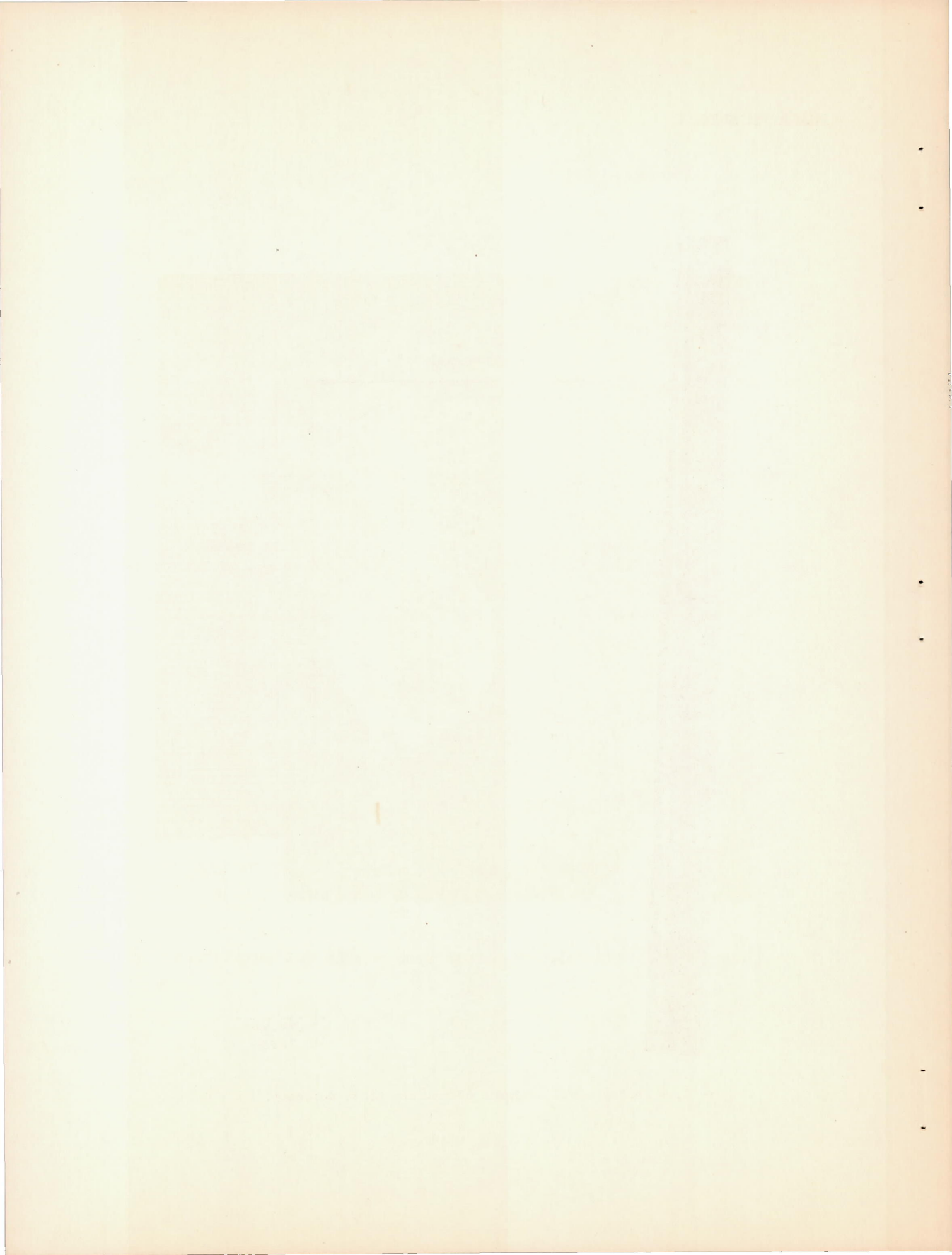


Figure 2. - Photographic evidence of uniform flame velocity.



NACA RM E50G24

1382

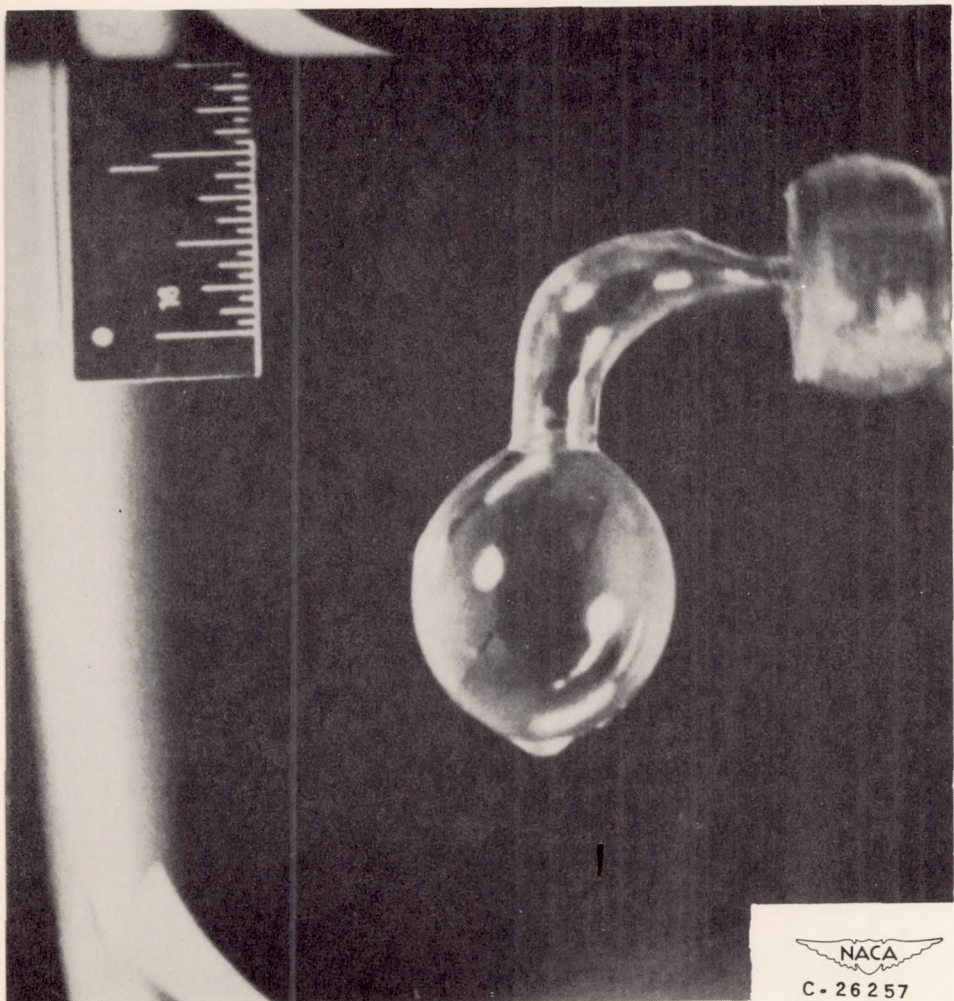
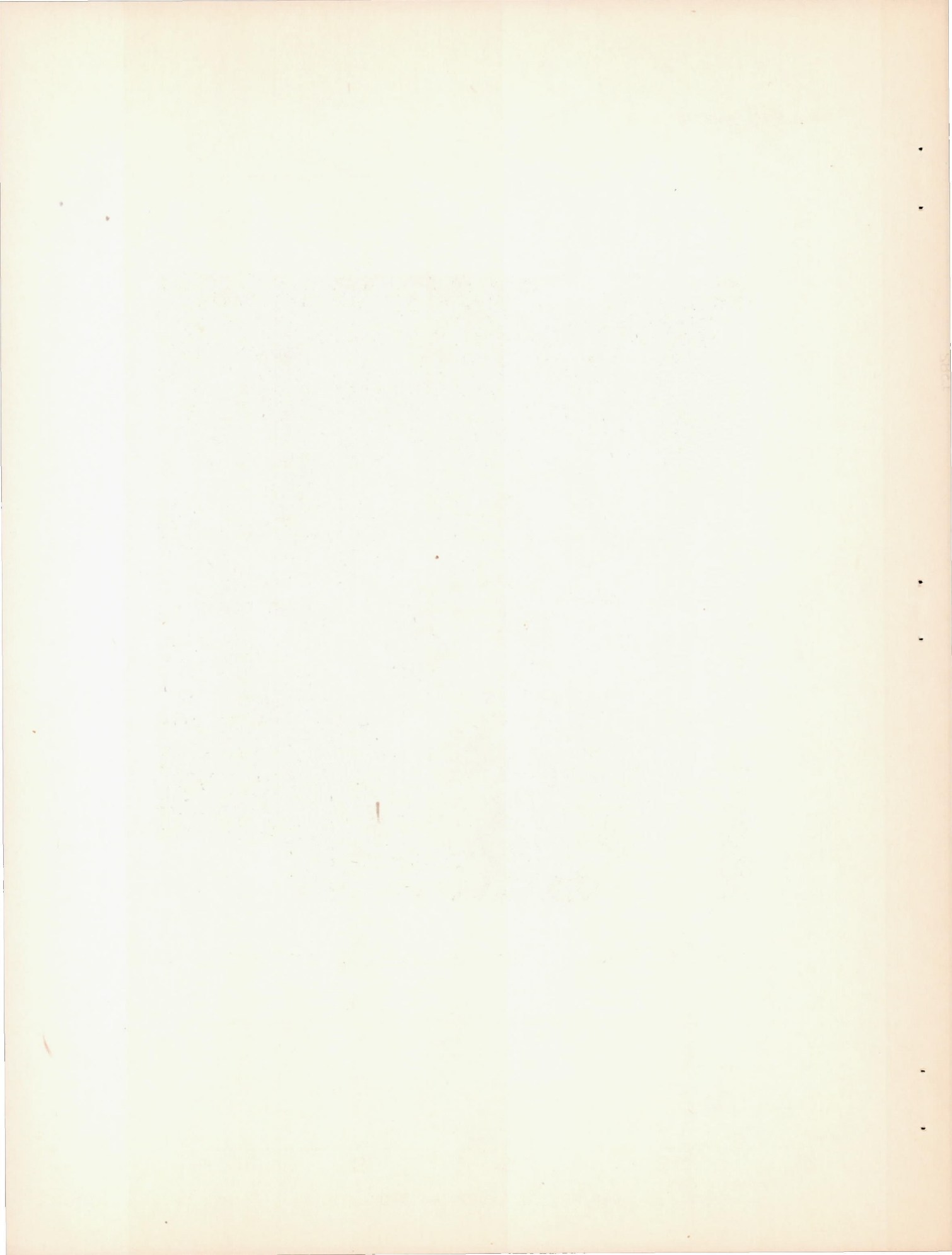


Figure 3. - Typical frame from soap-bubble motion picture.

NACA  
C-26257



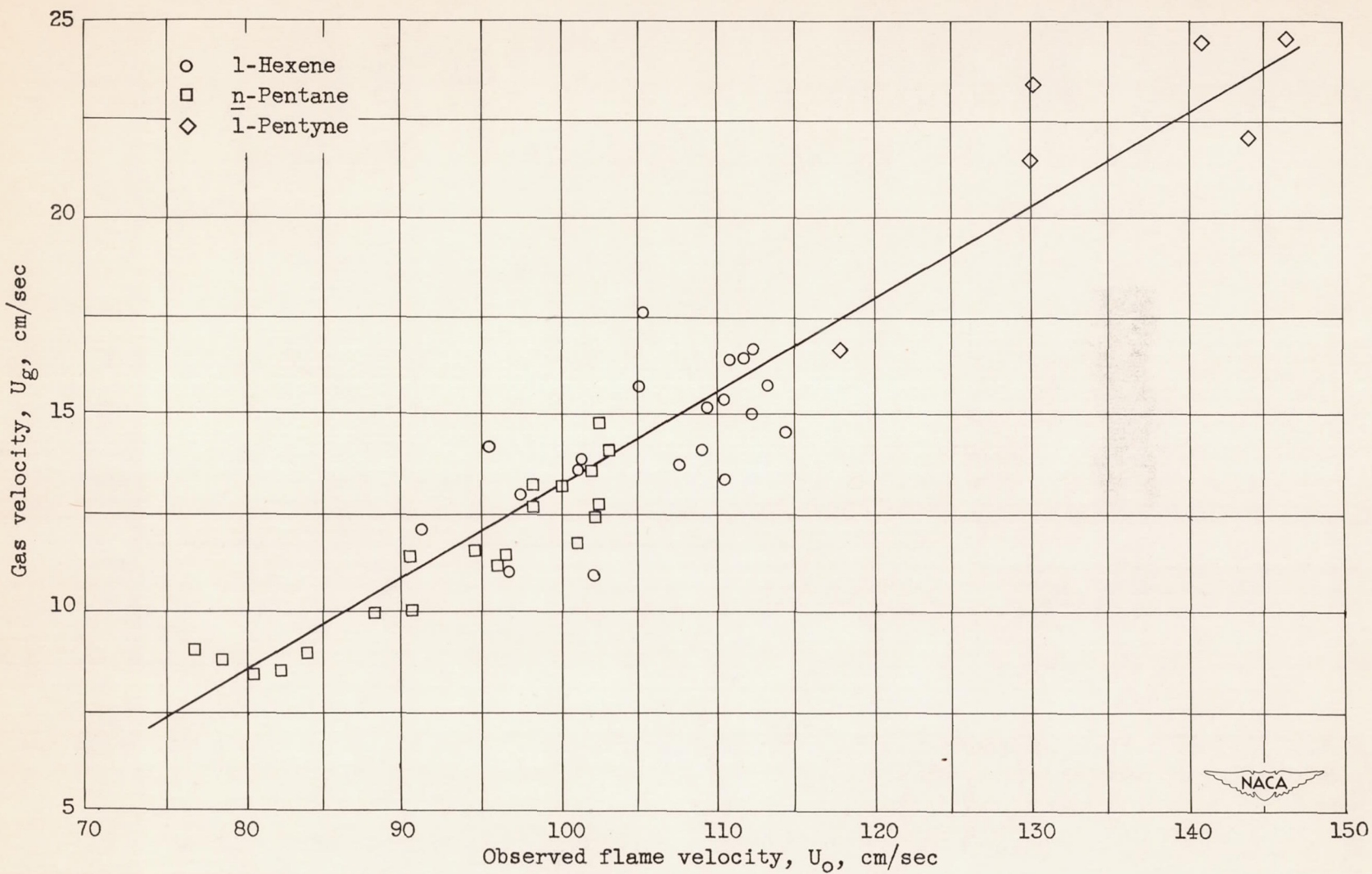
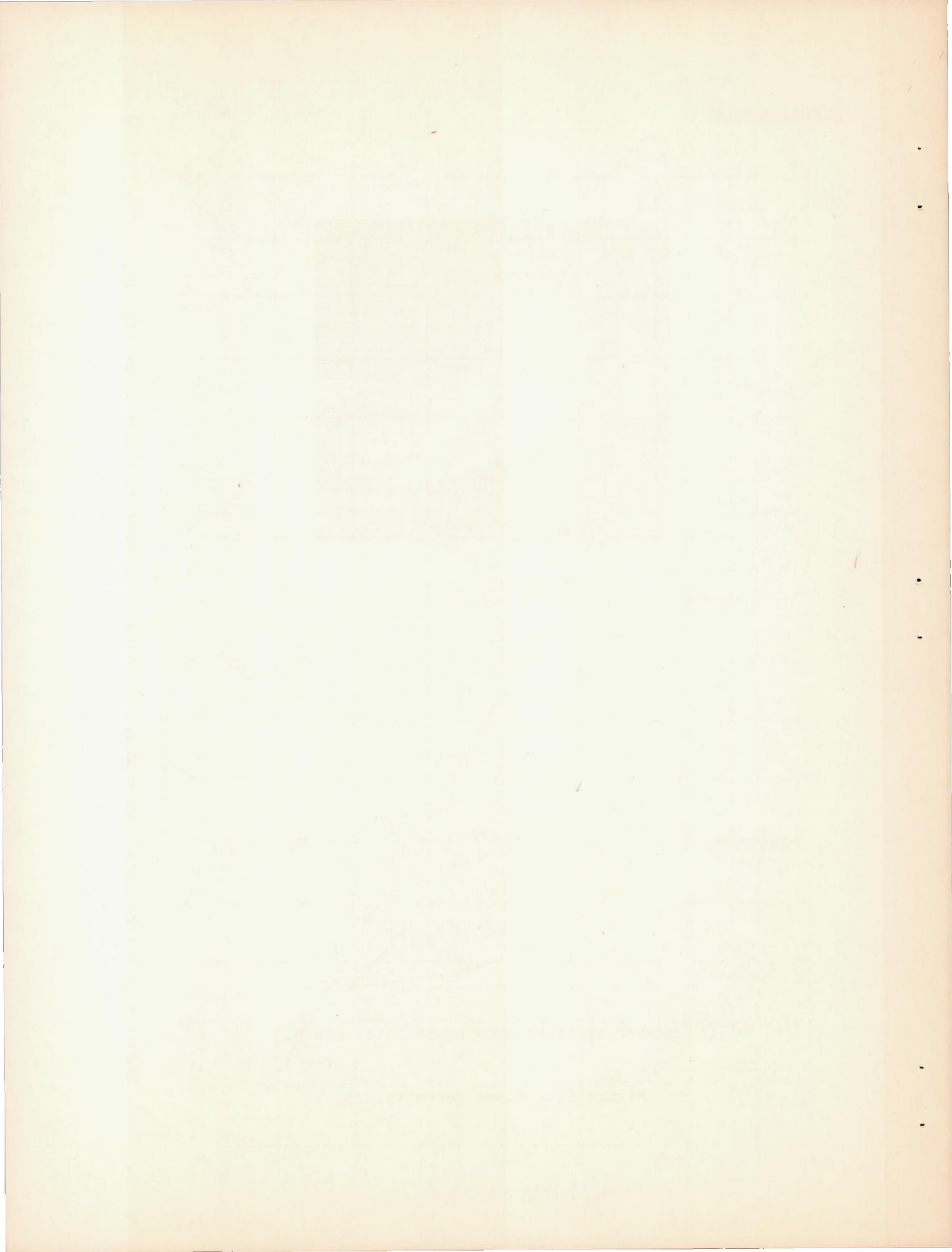


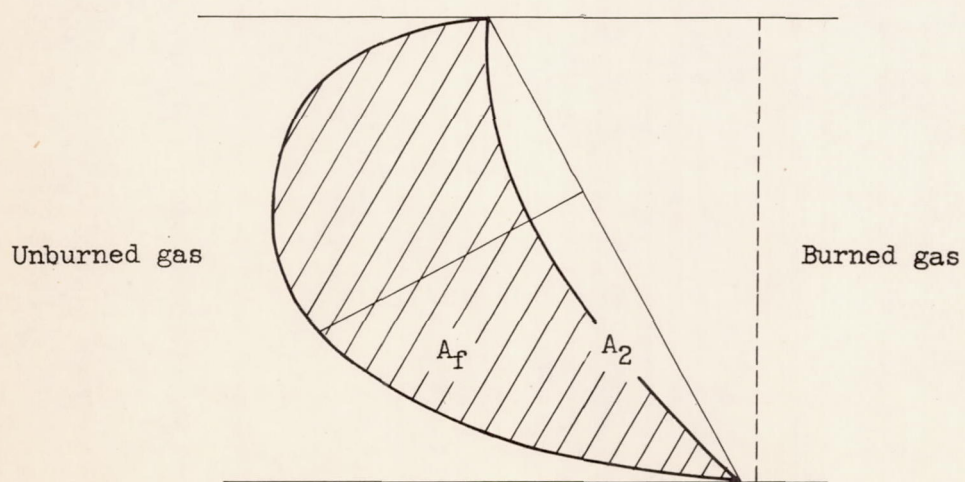
Figure 4. - Variation of unburned-gas velocity with observed linear flame velocity.





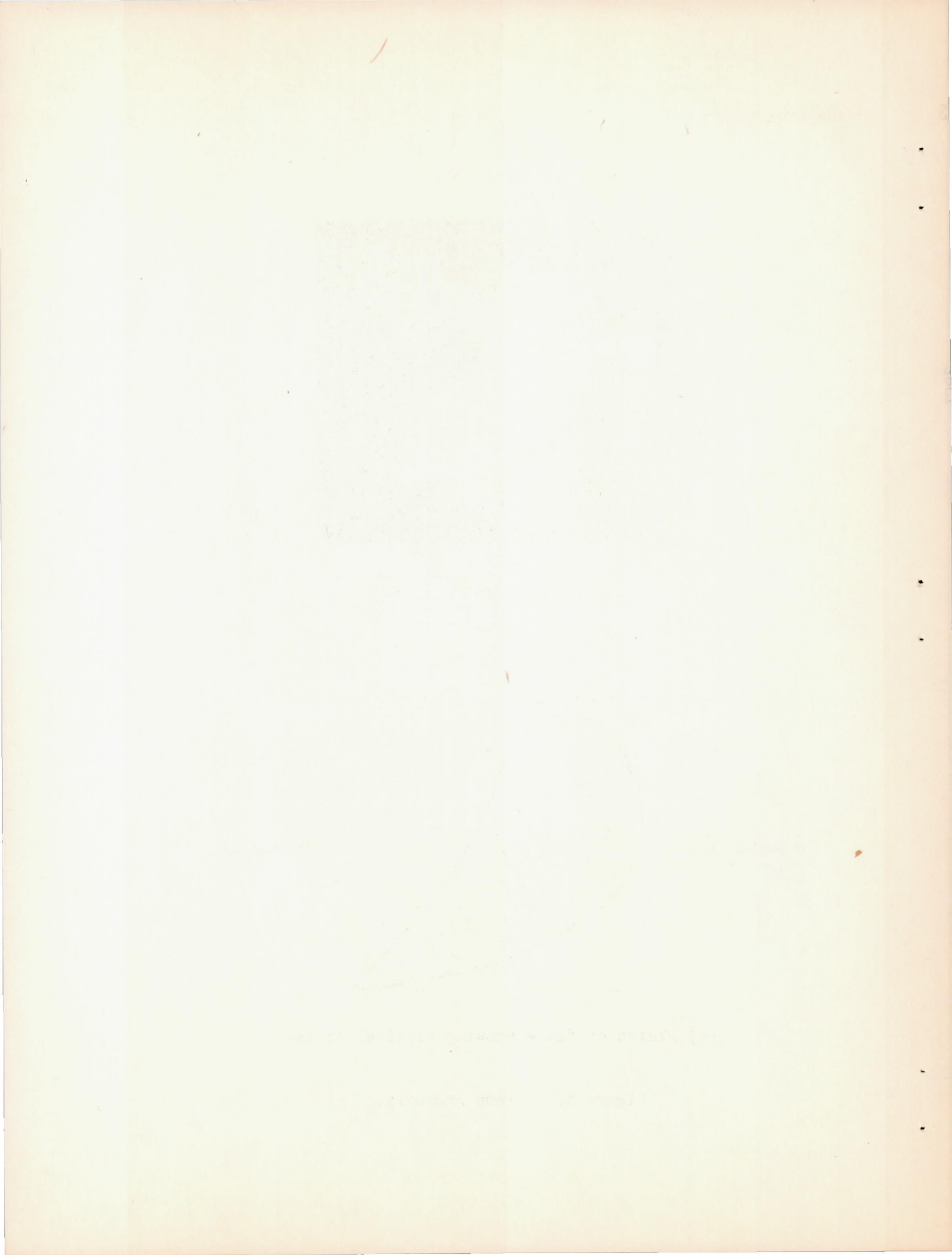
NACA  
C-26258

(a) Photograph of flame.



(b) Sketch of flame showing critical areas.

Figure 5. - Flame geometry.



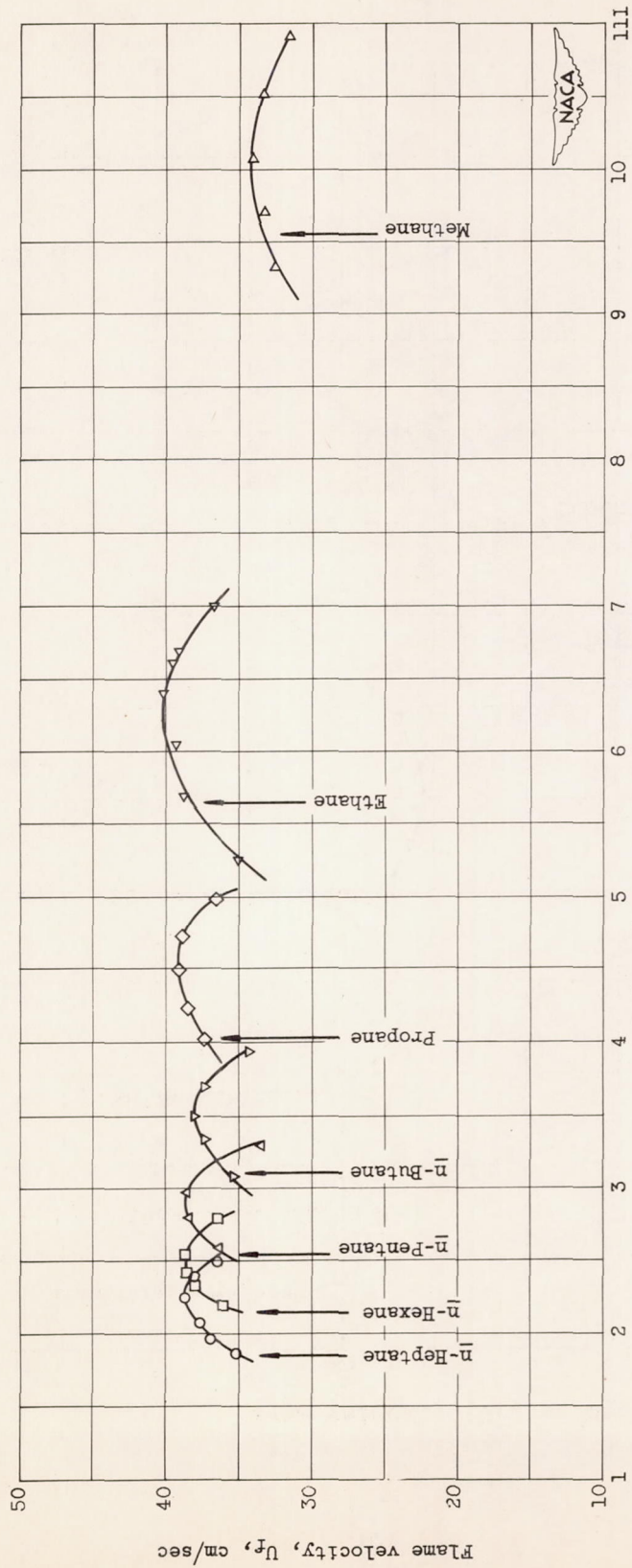


Figure 6. - Fundamental flame velocities of n-alkanes. Arrows indicate stoichiometric concentration.

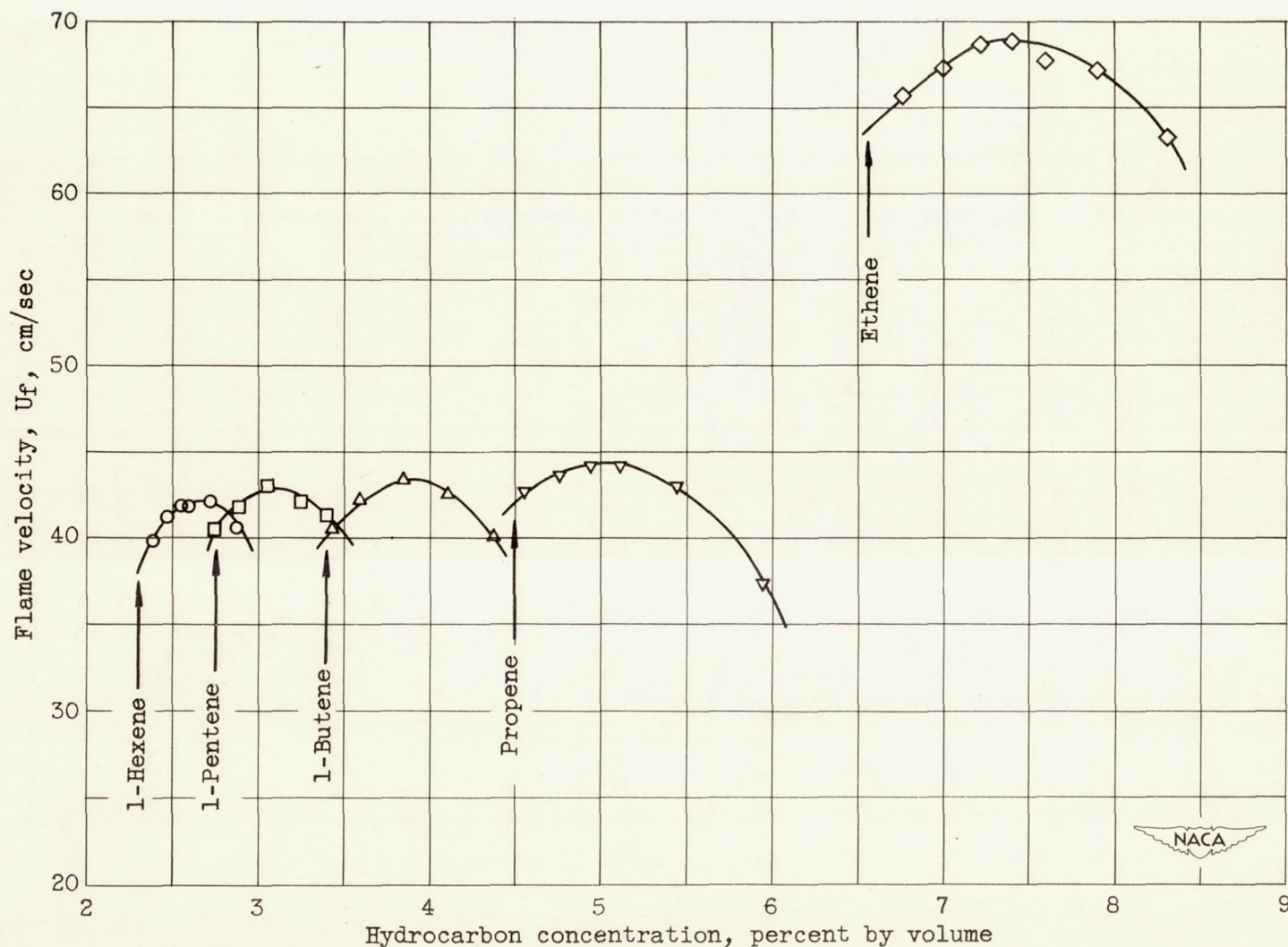


Figure 7. - Fundamental flame velocities of normal 1-alkenes. Arrows indicate stoichiometric concentration.

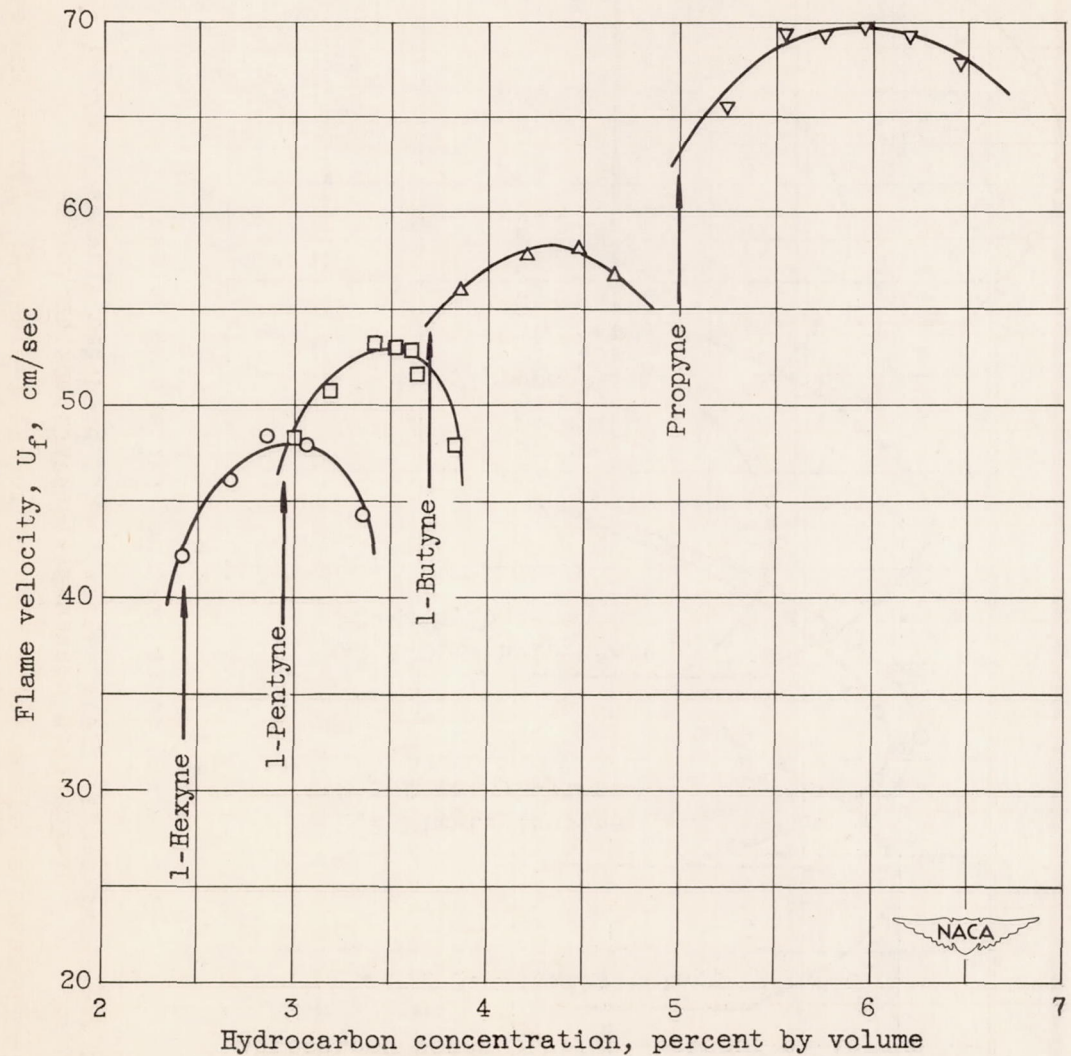


Figure 8. - Fundamental flame velocities of normal 1-alkynes.  
Arrows indicate stoichiometric concentration.

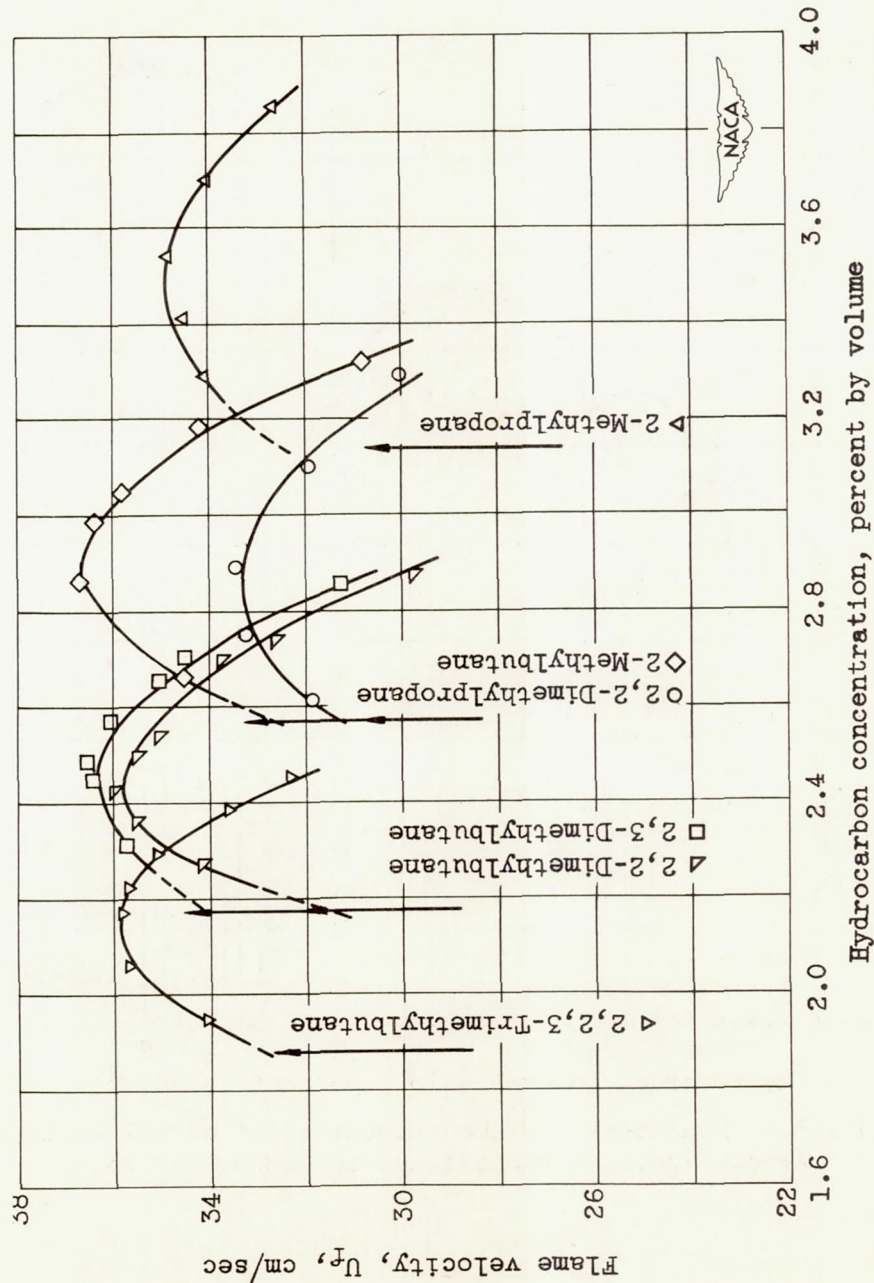


Figure 9. - Fundamental flame velocities of branched alkanes. Arrows indicate stoichiometric concentration.

1282

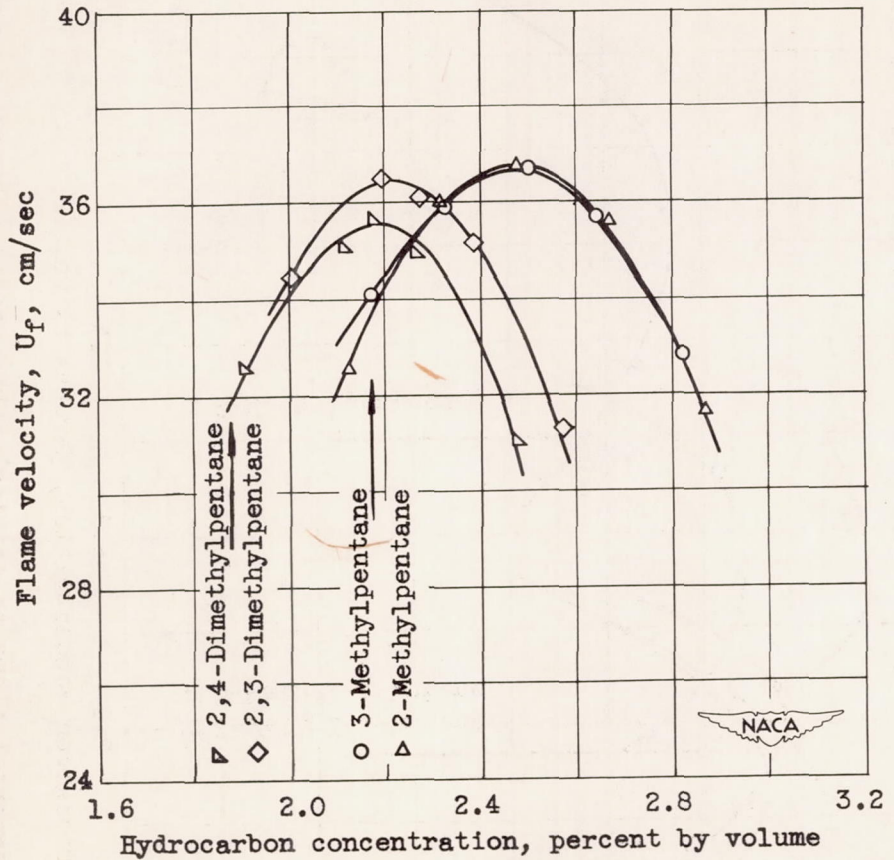


Figure 10. - Fundamental flame velocities of the branched alkanes. Arrows indicate stoichiometric concentration.

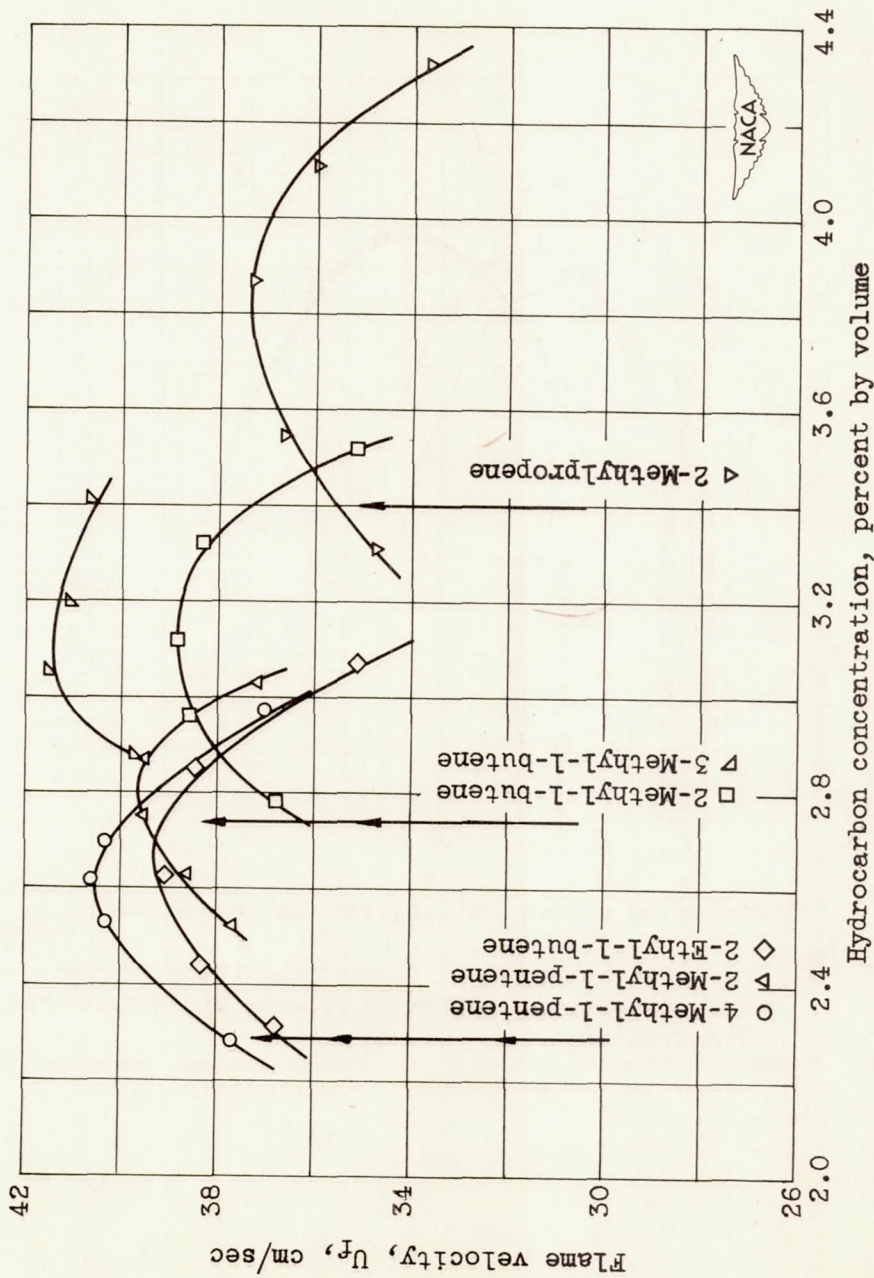


Figure 11. - Fundamental flame velocities of branched 1-alkenes. Arrows indicate stoichiometric concentration.

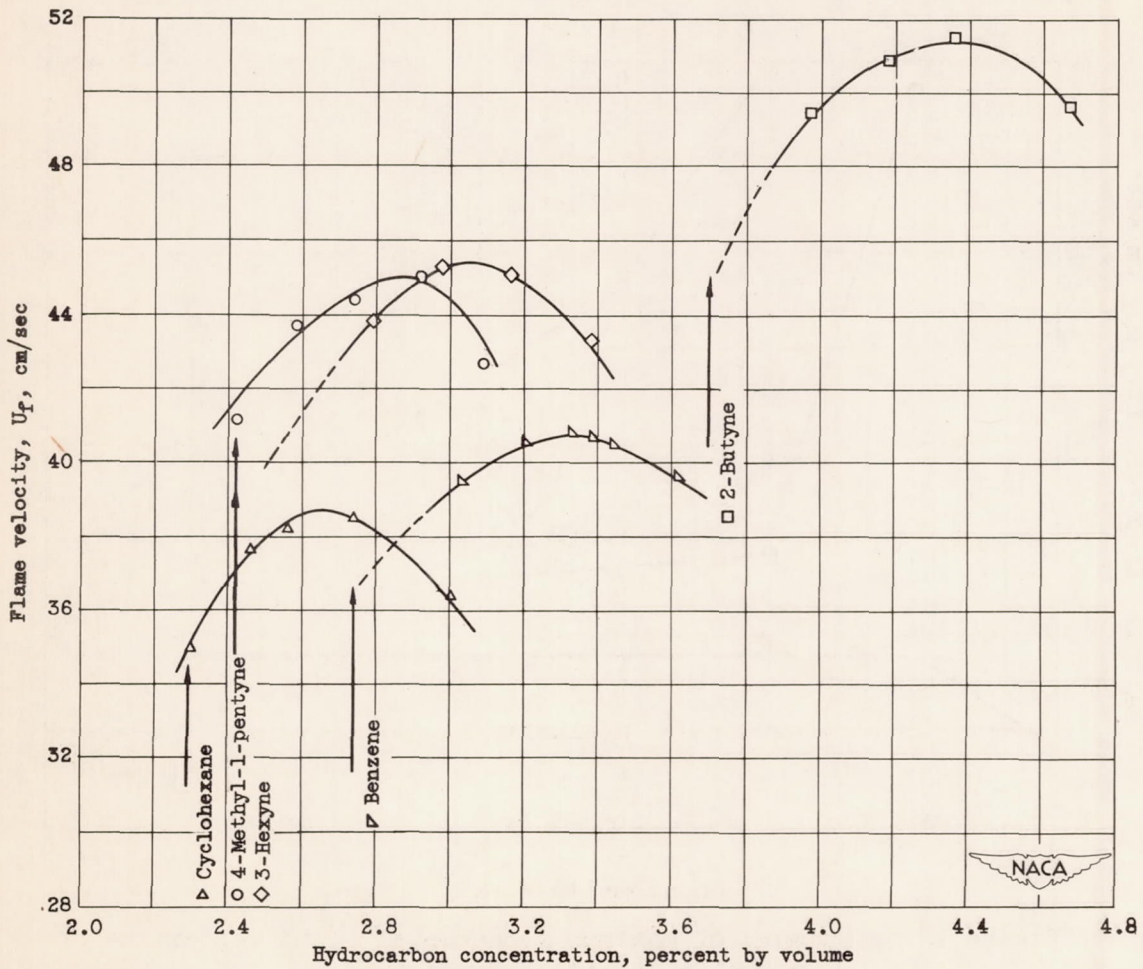


Figure 12. - Fundamental flame velocities of cyclohexane, benzene, and other alkynes.  
Arrows indicate stoichiometric concentration.

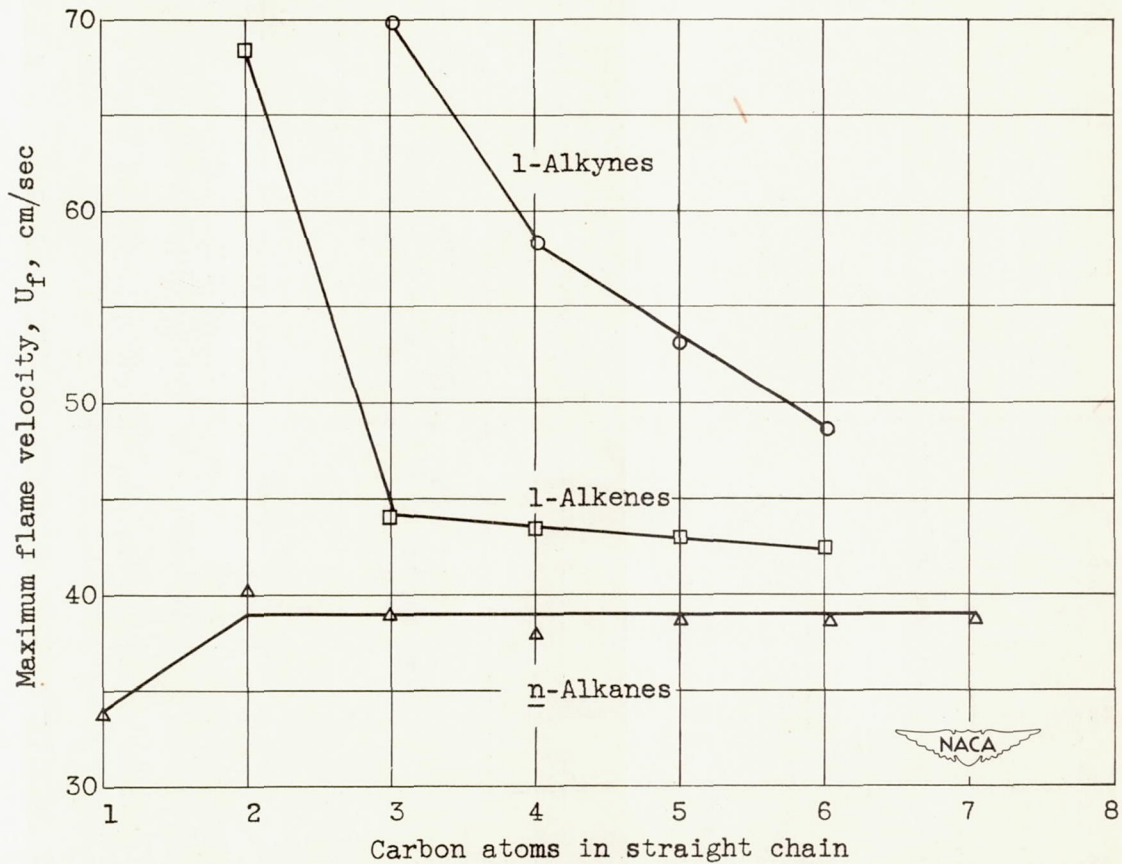


Figure 13. - Summary of maximum fundamental flame velocities of normal aliphatic hydrocarbons.

1382

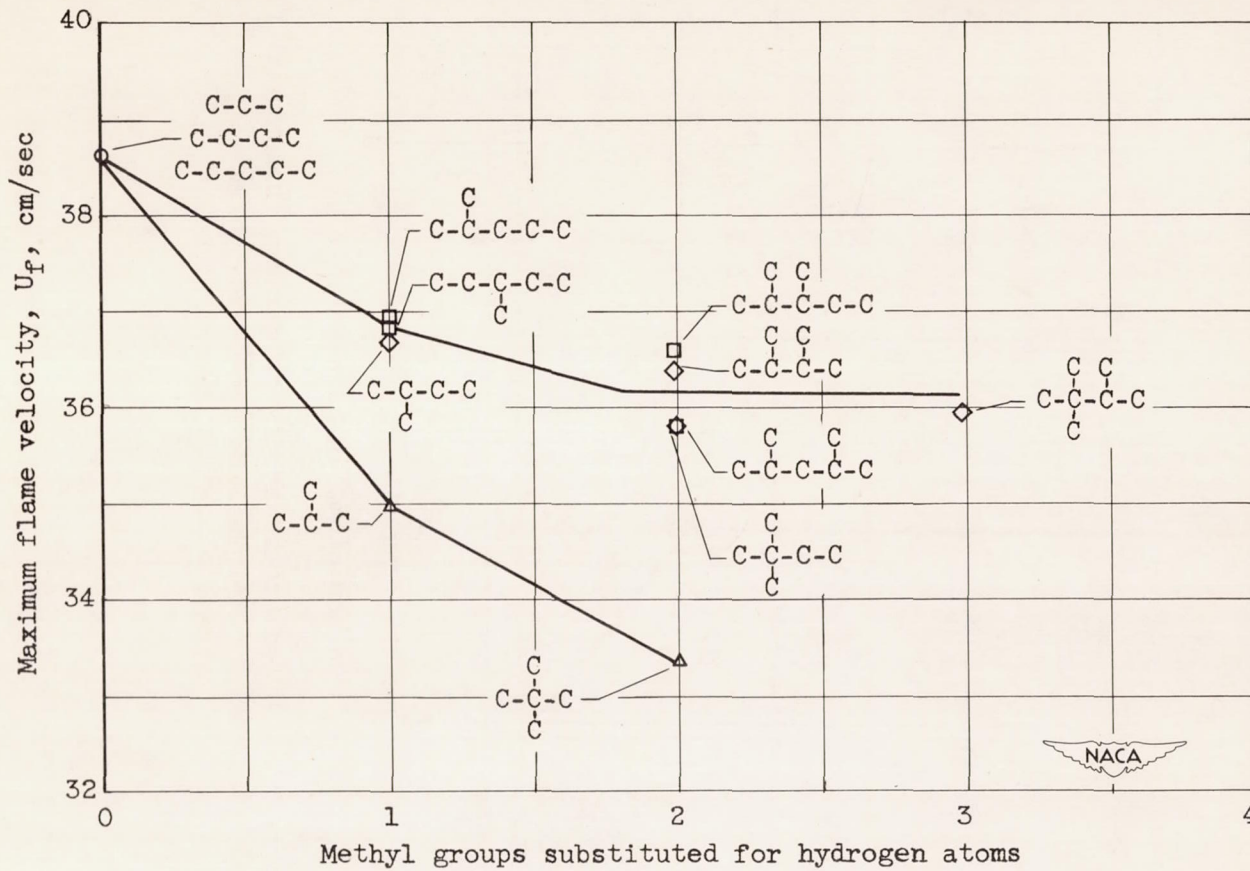


Figure 14. - Effect of branching on maximum fundamental flame velocity of alkanes.

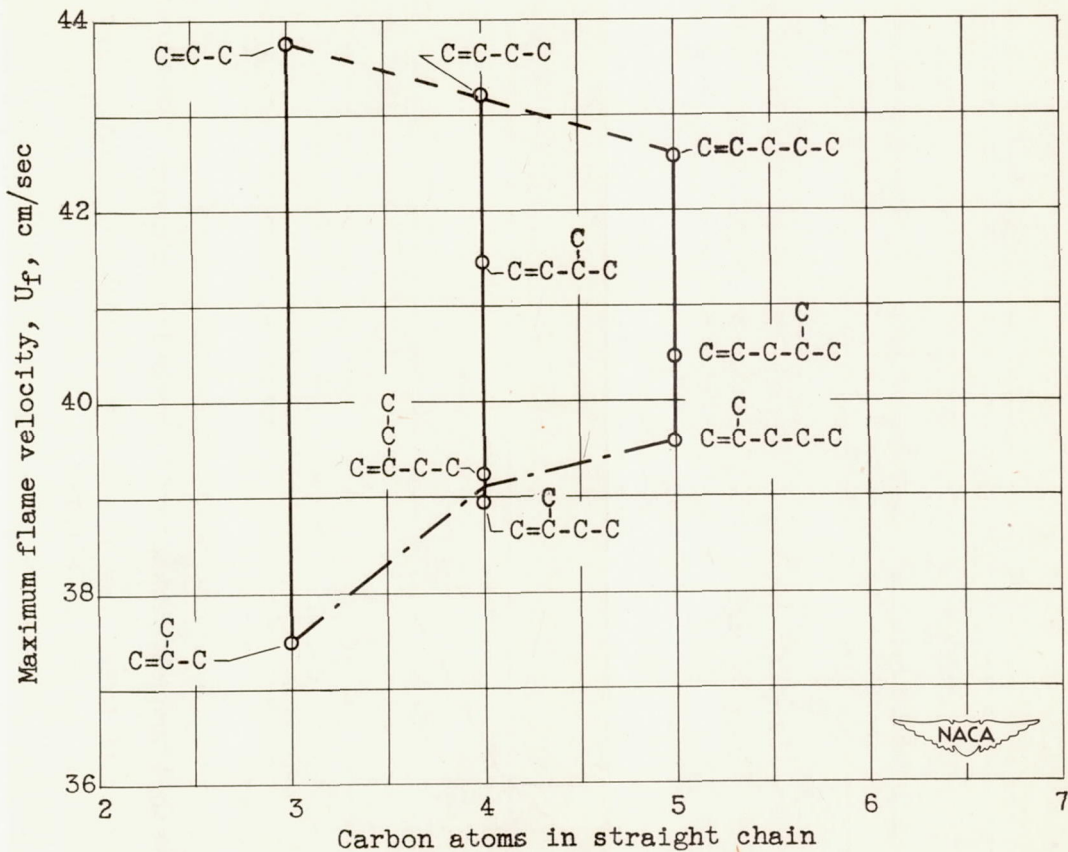


Figure 15. - Effect of branching on maximum fundamental flame velocity of 1-alkenes.